Transportation Infrastructure Restoration Optimization Considering Mobility and Accessibility in Resilience Measures

Tingting Zhao[1,2]
[1] University of Maryland, College Park
[2] Engineering Laboratory, National Institute of Standards and Technology
0107 Chemistry Building, 8051 Regents Dr, College Park, MD 20742
Email: tzhao1@umd.edu

Yu Zhang[3,*]
[3] Department of Civil and Environmental Engineering
University of South Florida (USF)
4202 E Fowler Ave, Tampa FL 33620
Email: yuzhang@usf.edu
Tel: 813-974-5846; Fax: 813-974-2957

* Corresponding Author

Submission Date: **April 2020**

ABSTRACT

Disruptive events lead to capacity degradation of transportation infrastructure, and a good restoration plan could minimize the aftermath impacts during the recovery period. This is considered one aspect of resiliency for transportation systems. Although unmet demand has been proposed as one measure of resilience for freight transportation, it has rarely been used for general transportation systems. This study takes unmet demand and total travel time as two measures in modeling the restoration plan problem and proposes a bi-objective bi-level optimization framework to determine an optimal transportation infrastructure restoration plan. The lower-level problem uses Elastic User Equilibrium to model the imbalance between demand and supply and measures the unmet demand for a given transportation network. The upper-level problem, formulated as bi-objective mathematical programming, determines optimal resource allocation for roadway restoration. The bi-level problems are solved by a modified active set algorithm and a network representation method derived from Network Design Problems. The Weighted Sum Method is adopted to solve the Pareto Frontier of this bi-objective optimization problem. The proposed restoration plan optimization method was applied to a typical road network in Sioux Falls, to verify the effectiveness of the methodology. For a given failure scenario, the Pareto Frontier of this bi-objective bi-level optimization problem with various budget levels, cross-referring to the travel efficiency of each solution, was illustrated to demonstrate how the proposed method can support decision-making for road network restoration. To further study the performance of the proposed method, different scenarios were generated with one to five links disrupted and the proposed methodology was applied with different budget levels. The statistical analysis of the optimized solutions for these scenarios demonstrates that a higher budget could help reduce unmet demand in the system by providing more restoration options.

Keywords: Transportation system resilience, Bi-level optimization, Bi-objective optimization, Elastic User Equilibrium, Criteria space analysis

1. Introduction

The resilience of Critical Infrastructure (CI) is essential for society to resist, respond to, and recover from disruptive events. A transportation system is one of 16 CI systems identified by Presidential Policy Directive 21 (White House, 2013). Efficient operation of a transportation system is particularly important in alleviating the impacts of disruptive events, and the repair and reconstruction of transportation infrastructure consumes tremendous material and human power; for example, Hurricane Katrina was estimated to cost more than $32 billion for the restoration of transportation infrastructure. Therefore, the effective planning of transportation infrastructure restoration tasks and resource allocation are of great concern for rapid and cost-efficient recovery in the aftermath of disruptive events. This work focuses on the restoration stage of a transportation system to provide effective decision-making methodologies to improve system resilience.

In proposing decision-making methods acting as force multipliers for effective system restoration, the first step is to determine the measurement of restoration work effectiveness. In this study, both total travel time and unmet demand in a transportation system are considered as resilience measures. A disruptive event such as an earthquake, flood, hurricane, landslide, or malicious act could lead to capacity degradation for some links and complete cutoff for others. This leads to increased travel time for some travelers compared to normal days. Furthermore, due to capacity degradation or loss, partial travel demand cannot be served by a devastated road network, termed as unmet demand, which has a serious impact on travelers, regulatory agencies, and industries.

Unmet demand has not been properly considered or included in most resilience measures in the existing literature. As one of the few works considering travel demand that cannot be served after a disruptive event, Chen and Miller-Hooks (2012) defined system resilience as demand that can be satisfied with a hard capacity constraint for the freight network flow model. In another work, Miller-Hooks et al. (2012) refined the aforementioned model and followed the same resilience measure based on unmet demand for freight transportation with further consideration of the balance between funds allocation to preparedness and recovery activities. However, network-wide traffic flow modeling and the strength of capacity constraint of freight transportation are essentially different from those of a general transportation system. (For more details about these differences, see Section 2). Therefore, although the concept of unmet demand can be borrowed from freight transportation literature, the methodology to quantify unmet demand and then measure system resilience accordingly is not applicable in this work. In addition to freight transportation system resilience analysis, unmet demand has been used in network-wide system performance evaluation and strategy optimization during the evacuation stage (Naghawi & Wolshon, 2014). However, the time scale and objective functions of evacuation problems are different from those of the restoration planning problem.

In this work, a bi-objective bi-level optimization problem was formulated to enhance transportation system resilience in the restoration phase after a disruptive event. This phase is different from the response phase shortly after the disruptive event. During the restoration phase, the infrastructure is waiting for repair, but daily travel demand has recovered to a relatively normal level, although some demand cannot be satisfied by the degraded infrastructure network, i.e., unmet demand. In reality restoration tasks could have multiple capacity recovery levels corresponding to various resource consumption (Vugrin et al., 2014), partially due to limited budget and resources and the need to restore multiple road sections to serve regional needs. In this study, the objective of the upper-level problem is to minimize total travel time and to minimize unmet demand by determining road sections to be restored and corresponding capacity recovery levels. The lower-level problem is to model road user travel behavior and address the imbalance between degraded supply and recovered demand of the transportation system after the event. Elastic User Equilibrium (EUE) traffic assignment is applied to this circumstance to provide network-flow assignment that result as input for the upper-level problem. The bi-level formulation serves as a constituent part for the overall bi-objective bi-level problem formulation. The Weighted Sum Method was adopted to solve the formulated bi-objective bi-level problem iteratively.

The remainder of this paper is organized as follows. Section 2 includes a thorough literature review that focuses on various resilience measures and the intrinsic connection and difference between the Network Design Problem (NDP) and the Restoration Plan Optimization (RPO) problem. Section 3 presents the bi-objective bi-level optimization formulation of the RPO problem and minimizes the two aspects, i.e., total travel time and unmet demand, as two objective functions. Section 4 proposes the solution algorithm for the optimization problem, and Section 5 applies the RPO method to a typical road network to illustrate the implementation procedures, verify the effectiveness of this method, and further interpret the empirical analysis results from a criteria space analysis perspective for the bi-objective optimization. Results clearly show how the two different optimization objectives (minimize total travel time and minimize unmet demand) trade off with each other and how the budget for restoration work could influence optimization results. The last section summarizes the contributions of this work and discusses future research directions.

2. Literature Review

2.1. Resilience Measurement

There are two types of resilience measures for transportation systems, network topology-based and system performance-based. Network topology-based measures include origin-destination (O-D) connectivity (Zhang et al., 2015a), average reciprocal distance (Zhang et al., 2015a), average degree (Leu et al., 2010; Zhang et al., 2015a), diameter (Zhang et al., 2015a), cyclicity (Zhang et al., 2015a), betweenness (Leu et al., 2010), network coverage (Chang and Nojima, 2001), and travel alternative diversity (Xu et al., 2015). System performance-based measures include travel time, travel cost, and environmental factors (Omer et al., 2013), travel demand (Chen and Miller-Hooks, 2012; Miller-Hooks et al., 2012), and consumer surplus-based (Soltani-Sobh et al., 2015) resilience measures. As both total travel time and unmet demand are considered to evaluate the restoration plan in this research effort, it falls into the system performance-based resilience measures category.

Among these existing system performance-based resilience measures, travel time-based measures are the most widely applied (Faturechi and Miller-Hooks, 2015; Morohosi, 2010; Zhang et al., 2015a). For instance, Faturechi and Miller-Hooks (2014) defined resilience as the network's ability to resist and adapt to disruption, with total travel time employed in assessing system resilience. As illustrated in Fig. 1, system resilience is measured by travel time resilience, $R_{T,B}$, which is formulated as the reciprocal of total travel time at the end of the response stage (tt_f) divided by the reciprocal of total travel time at the time just before the event occurred (tt_0). System resilience optimization methods with the objective to maximize travel time-related measures were proposed accordingly (Faturechi and Miller-Hooks, 2014), which aid decision-makers from a mobility perspective.

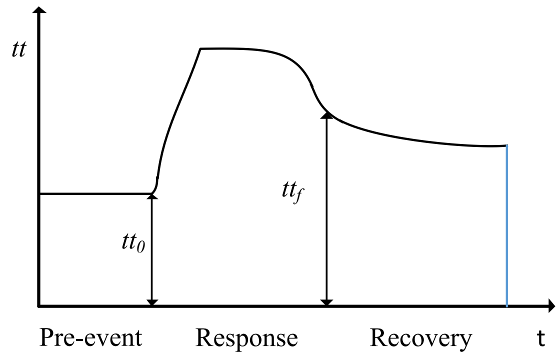

Fig. 1. Travel time-based resilience measures.

* tt_0 and tt_f: total travel times at the end of pre-event and response stages (Faturechi and Miller-Hooks, 2014)

However, after catastrophic events such as flood or earthquake, roadway performance can be seriously affected, with huge capacity reduction of links and total loss of some links. There exists the possibility that partial travel demand cannot be accommodated by the degraded transportation system, and unmet demand has a critical impact on system level of service. Therefore, evaluation of network resilience performance without considering unmet travel demand can be biased and may lead to less cost-effective restoration plan results. To evaluate total travel time and unmet demand, it is necessary to properly model traffic flow assignment to capture the travel behavior to be integrated into system level performance representation. Until 2005, all previous resilience studies lacked consideration of traffic flow assignment mechanism. This gap was addressed in a study by Murray-Tuite (2006), in which a measure of transportation system resiliency was introduced and was composed of 10 dimensions, i.e., redundancy, diversity, efficiency, autonomous components, strength, collaboration, adaptability, mobility, safety, and the ability to recover quickly. The influence of traffic assignments, both system optimal and user equilibrium, were examined on four dimensions of the resilience measurement. In the present work, to model the imbalance between supply and demand more specifically, Elastic UE is adopted to capture traveler behavior and support the calculation of total travel time and unmet demand.

The concept of unmet demand has been applied in freight transportation system resilience analysis and optimization. For example, Miller-Hooks et al. (2012) defined system resilience as demand that can be satisfied with a hard capacity constraint for the freight network flow model. However, the traffic flow assignment mechanism and the strength of capacity constraint of freight transportation are essentially different from those of a general transportation system. The network flow models for freight transportation system resilience analysis in Chen and Miller-Hooks (2012) and Miller-Hooks et al. (2012) were formulated as maximum flow problem (Liu and Mu, 2015; Righini, 2016). However, the network flow model for general traveler transportation systems applies either user equilibrium or system optimum. The other difference between freight transportation and general transportation problem formulation is capacity constraint. Capacity constraints for most freight transportation flow assignment models are hard capacity constraints, restricting flow on each arc to be less than the capacity (for example, Chen and Miller-Hooks, 2012, and Miller-Hooks et al., 2012). In general transportation network design or operational optimization problems, traffic flow assigned on a link is allowed to be larger than the capacity, and the link performance function (such as the Bureau of Public Roads [BPR] function) is used to calculate the travel time of the link. Therefore, capacity constraint for the general traffic flow assignment model is a relatively soft constraint.

In addition to freight transportation system resilience analysis, the concept of unmet demand has also been used in network-wide system performance evaluation and strategy optimization during the evacuation stage (Zhang et al., 2015b). For instance, Xie et al. (2010) used "percentage of evacuees arrived at destination" curves to evaluate system performance under different evacuation strategies. More recently, Zhang et al. (2015b) and Zockaie et al. (2014) leveraged the macroscopic productivity function—the Macroscopic Fundamental Diagram (MFD)—to perform network performance evaluation for evacuation strategy optimization. To reduce the likelihood of over-saturation in a transportation network during evacuation, an optimization model was proposed in Zhang et al. (2015b) to maximize evacuation throughput traffic for regional networks. The difference between transportation network performance analysis during the evacuation and restoration stages stems from both the time scale and the main concerns for performance evaluation. The evacuation stage is much shorter than the restoration stage; therefore, although mobility, accessibility, safety, etc., are common perspectives for performance evaluation of different stages, the evacuation stage performance evaluation needs more dynamic information due to a shorter time period and highly unstable system performance (Dixit and Wolshon, 2014). Therefore, most studies applied dynamic traffic assignment or traffic simulation to obtain dynamic traffic information for system performance evaluation during the evacuation stage (Cova and Johnson, 2002; Jahangiri et al., 2014; Lim and Wolshon, 2005; Murray-Tuite and Mahmassani, 2004; Murray-Tuite, 2006; Naghawi and Wolshon, 2010; Wolshon et al., 2015; Wolshon, 2009). This work focuses on the restoration stage (part of the recovery stage) of a transportation system when the infrastructure is still damaged or disrupted but daily travel demand has recovered to a relatively normal level. As the restoration stage has a longer time scale, a more macroscopic network flow model (Elastic UE) is adopted to obtain traffic flow information for restoration performance evaluation.

In addition to the literature in the context of freight transportation and evacuation, Nogal et al. (2016) and Nogal et al. (2017) analyzed the impact of demand variation on transportation network resilience. However, system resilience in those studies was quantified by travel time increase and traffic flow variations in the system without involving unmet travel demand.

In summary, there have been extensive studies on transportation system resilience, and some researchers proposed to consider unmet demand in the context of freight transportation or evacuation strategy optimization. However, the problem setting, modeling, and system performance evaluation are different from a general transportation system in the context of restoration plan optimization. Therefore, in this study, we propose to enhance transportation system resilience in the restoration stage in terms of both mobility (to reduce total travel time) and accessibility (to reduce unmet demand) through a bi-objective bi-level problem formulation. As the constituent bi-level problem formulation is similar to the Network Design Problem (NDP), the literature on NDP was briefly reviewed; the connection and difference between the NDP and RPO problems are described in the next subsection.

2.2. Connection and Difference between NDP and RPO Problems

The RPO problem is a type of NDP under special circumstances. The objective of a typical NDP is to make investment decisions to optimize a given system performance measure, such as total travel cost in a network, while accounting for the route choice behavior of network users (Yang and Bell, 1998). Due to the complexity of problem formulation and computational challenges, NDP has been recognized as one of the most difficult problems in the transportation area. However, as NDP has great potential for solving planning, design, and congestion pricing problems, it has drawn abundant attention and effort from the transportation research community (Boyce and

Janson, 1980; Mingyuan and Attahiru Sule, 1991; Zhang et al., 2009a). NDP has been classified into two different forms—Discrete NDP (DNDP), concerning the addition of new links to an existing road network (Boyce and Janson, 1980; Mingyuan and Attahiru Sule, 1991; Zhang et al., 2009a), and Continuous NDP, concerning the optimal capacity expansion of existing links (Friesz, 1985; Hai, 1995). DNDPs are modeled as nonlinear integer programming models constrained with network equilibrium. Typical DNDP solution algorithms include Bender's decomposition, branch-and-bound methods, and heuristics.

NDP and RPO problems have some similarities. As road section capacities decrease after an earthquake, flood, or hurricane, the imbalance between network-wide transportation service supply and travel demand emerges. This is similar to the imbalance between transportation service supply and travel demand caused by economic growth and land use relocation in NDP. However, these two problems are also different. As previously noted, the cause of the imbalance between transportation service supply and travel demand is different for NDP and RPO problems. Furthermore, the magnitude of the short-term impact of natural disasters on the network can be much more intense than the short-term impact of economic growth and land use relocation. Due to sudden capacity degradation or loss, there is sharp imbalance between supply and demand after disruptive events, leading to partial travel demand that may not be served by the devastated road network. To recover from catastrophic events, a basic concern of restoration is reducing unmet demand in the system. Therefore, the objective of RPO is to reduce not only total travel time but also unmet demand. Consequently, the tradeoff between reducing total travel time and unmet demand should be taken into account in RPO problem formulation.

The following sections propose a bi-objective bi-level formulation to solve the RPO problem for a transportation system to enhance both mobility (by minimizing total travel time) and accessibility (by minimizing unmet demand). The bi-objective problem is solved by the Weighted Sum Method and the componential bi-level problems (to minimize the two objectives respectively or to minimize the combination of them) is solved by a modified active set algorithm and a network representation method.

3. Restoration Plan Optimization Problem Formulation

3.1. Two Resilience Measures—Total Unmet Demand and Total Travel Time

As noted, existing research efforts involving unmet demand in resilience analysis are not sufficient to draw firm conclusions about how to improve system resilience accordingly, especially for a general transportation system in the restoration stage. To address this issue, the following two resilience measures are proposed in terms of both total unmet demand and total travel time:

$$\begin{aligned} R_1 &= D = \sum_{rs} \hat{D}_{rs} \\ R_2 &= T = \sum_{a} x_a^* \cdot t_a(x_a^*, c_a) \end{aligned} \tag{1}$$

where $D = \sum_{rs} \hat{D}_{rs}$ defines total unmet demand in the system and $T = \sum_{a} x_a^* \cdot t_a(x_a^*, c_a)$ defines total travel time in the system (x_a^* is the equilibrium flow on link a, c_a is the capacity for link a). The unmet demand is quantified by the elastic demand traffic assignment model, as elaborated in Section 3.3. These two resilience measures contradict each other; therefore, a bi-objective optimization problem formulation is adopted to tackle the RPO problem with two contradicting objectives given that these two objectives have different units, i.e., travel time and number of trips not satisfied by the infrastructure system.

3.2. Formulation of RPO as a Bi-objective Bi-level Optimization Problem

Taking the proposed resilience measures as the two objective functions, restoration plan optimization after a disruptive event is formulated as a bi-objective bi-level optimization problem. The bi-level problem serves as the building-block for the overall problem formulation. Bi-level optimization is also known as the Stackelberg leader-follower problem, which represents a situation involving two decision-makers, with the behavior of the leader influencing the follower's choice. In this problem, the upper-level decision-maker is a city administrator who decides which road sections of the network will be repaired after the event given a limited budget. The lower-level decision-makers are road users who are affected by road network capacity degradation or link loss due to the event. As the restoration plan changes the road capacity, it alters the network-wide level of service that will influence a traveler's decision-making; given the restoration plan, updated traveler decisions result in re-assigned traffic flows on the restored transportation network and corresponding system performance after the restoration effort. This updated network-wide system performance according to traveler decision-making is taken into account for the city administrator's decisions in terms of the restoration planning. Therefore, a bi-level optimization problem is appropriate for modeling the RPO building-block problem. The formulation of the overall bi-objective bi-level RPO problem proposed in this work is illustrated as follows.

Upper-level problem:

$$\min \begin{pmatrix} \sum_{rs} \hat{D}_{rs} \\ \sum_{a} x_a^* \cdot t_a(x_a^*, c_a) \end{pmatrix} \tag{2}$$

$$\text{s.t.} \sum_{a \in \bar{A}} M_{a,1} \cdot y_{a,1} + M_{a,2} \cdot y_{a,2} \le B \tag{3}$$

$$y_{a,1} + y_{a,2} \le 1, \forall a \in \bar{A} \tag{4}$$

$$y_{a,l} \in \{0,1\}, \forall a \in \bar{A}, l = 1, 2 \tag{5}$$

$$\text{where, } x_a^* = \arg\min \sum_a \int_0^{x_a} t_a\left(\omega, c_{a,0} + c_{a,1} y_{a,1} + c_{a,2} y_{a,2}\right) d\omega - \sum_{rs} \int_0^{q_{rs}} D_{rs}^{-1}(\omega)\, d\omega \tag{6}$$

$$\sum_{rs} \hat{D}_{rs} = \sum_{rs} f_{rs,p} \tag{7}$$

Lower-level problem:

$$\min \sum_a \int_0^{x_a} t_a\left(\omega, c_{a,0} + c_{a,1} y_{a,1} + c_{a,2} y_{a,2}\right) d\omega - \sum_{rs} \int_0^{q_{rs}} D_{rs}^{-1}(\omega)\, d\omega \tag{8}$$

$$\text{s.t.} \sum_k f_{rs,k} = q_{rs} \qquad \forall r, s \tag{9}$$

$$f_{rs,k} \ge 0 \qquad \forall k, r, s \tag{10}$$

$$q_{rs} \ge 0 \qquad \forall r, s \tag{11}$$

$$x_a = \sum_{rs} \sum_k f_{rs,k} \delta_{a,k}^{rs}, \forall a \tag{12}$$

Referring to Equation (2), the objective function of the upper-level problem is to minimize the two system resilience measures, i.e., total unmet demand and total travel time (note that in this study smaller resilience measurement indicates better resilience performance). The total budget for the whole restoration plan is restricted in constraint (3). Constraints (4) and (5) guarantee that for each candidate link, either restoration work with higher (level 1, $l=1$) or lower (level 2, $l=2$) resource consumption is adopted (when $y_{a,1}+y_{a,2}=1$) or no action is taken (when $y_{a,1}=0, y_{a,2}=0$). $t_a(x_a, c_a)$ in Equation (2) is the travel time function.

The Bureau of Public Roads (BPR) function is adopted as the travel time function in this work:

$$t_a(x_a, y_a) = t_a^0 \left\{ 1+0.15 \left[\frac{x_a}{c_a^0 + c_{a,1} y_{a,1} + c_{a,2} y_{a,2}} \right]^4 \right\} \tag{13}$$

Table 1 summarizes the notations used in the bi-objective bi-level problem formulation.

Table 1 Notations in proposed bi-objective bi-level problem formulation.

Notation	**Explanation**
a	Link index
x_a	Flow on link a; $\mathrm{X} = (\ldots, x_a, \ldots)$
t_a	Travel time on link a; $\mathrm{t} = (\ldots, t_a, \ldots)$
$c_{a,00}$	Original capacity of link a before disruptive event
$c_{a,0}$	Capacity of link a at the moment after disruptive event
$\bar{A}_1$	Candidate links with capacity augment level 1
$\bar{A}_2$	Candidate links with capacity augment level 2
$\bar{A}=\bar{A}_1 \cup \bar{A}_2$	All candidate links
$c_{a,1}, \forall a \in \bar{A}_1$	Capacity augment for link a with level 1
$c_{a,2}, \forall a \in \bar{A}_2$	Capacity augment for link a with level 2
$M_{a,1}, \forall a \in \bar{A}_1$	Cost for link a with capacity augment level 1
$M_{a,2}, \forall a \in \bar{A}_2$	Cost for link a with capacity augment level 2
$y_{a,l}, \forall a \in \bar{A}_1 \cup \bar{A}_2, l=1,2$	Binary variables, 1 indicates that corresponding plan is adopted, 0 means not
N	Node (index) set
A	Arc (index) set
K_{rs}	Set of paths connecting O-D pair $r-s$; $r \in \Re, s \in \Psi$
$f_{rs,k}$	Flow on path k connecting O-D pair $r-s$; then for each O-D pair $r-s$, $\mathrm{f}^{rs} = (\ldots, f_{rs,k}, \ldots)$; for all O-D pairs $\mathrm{f} = (\ldots, \mathrm{f}^{rs}, \ldots)$
$t_{rs,k}$	Travel time on path k connecting O-D pair $r-s$; $t^{rs} = (\ldots, t_{rs,k}, \ldots)$; for all O-D pairs $t = (\ldots, t^{rs}, \ldots)$
q_{rs}	Trip rate between origin r and destination s;

$\delta_{a,k}^{rs}$	$\delta_{a,k}^{rs}=\begin{cases}1 & \text{if link } a \text{ is on path } k \text{ between O-D pair } r\text{-}s\\ 0 & \text{otherwise}\end{cases}$ $\Delta^{rs}=\left(\ldots,\delta_{a,k}^{rs},\ldots\right)$ is for O-D pair $r-s$ $\Delta=\left(\ldots,\Delta^{rs},\ldots\right)$ is for all O-D pairs
u_{rs}	Minimum travel time between $r-s$
$D_{rs}(\cdot)$	Demand function between $r-s$
$D_{rs}^{-1}(\cdot)$	Inverse demand function between $r-s$
r	Origin node index
s	Destination node index
$t_{rs,p}$	Travel time on the pseudo link between O-D pair $r-s$
$f_{rs,p}$	Flow on pseudo link between O-D pair $r-s$
$\bar{D}_{rs}$	Total demand between O-D pair $r-s$ before special event
$\widehat{D}_{rs}$	Unmet demand between O-D pair $r-s$
T_0	Total Travel Time in the system before restoration
T_f	Total Travel Time in the system after restoration
$\hat{D}_0$	Total Unmet Demand in the system before restoration
$\hat{D}_f$	Total Unmet Demand in the system after restoration

3.3. Formulation of Lower-level Problem by EUE Model

For the lower-level problem, to quantify unmet travel demand, the EUE model (Daskin and Sheffi, 1985) was applied to depict traveler route choice behavior and address the imbalance between transportation service supply and travel demand.

Traditionally, NDP models assume that travel demand is given and fixed, and driver route choice behavior is characterized by a User Equilibrium (UE) problem (Yang and Bell, 1998). The UE problem with a fixed demand can be formulated as follows (Daskin and Sheffi, 1985):

$$\min z(x,q)=\sum_{a}\int_{0}^{x_a} t_a\left(\omega\right)d\omega \tag{14}$$

$$\text{s.t.}\sum_{k} f_{rs,k}=q_{rs} \qquad \forall r,s \tag{15}$$

$$f_{rs,k}\geq 0 \qquad \forall k,r,s \tag{16}$$

$$q_{rs}\geq 0 \qquad \forall r,s \tag{17}$$

However, as the NDP generally involves long-term investment in a road network that consequently influences travel demand in the system, assuming a given and fixed travel demand is not realistic. Therefore, the EUE model was developed to incorporate the elasticity of travel demand into the NDP (Gartner, 1980). In the EUE model, travel demand between an O-D pair varies with travel cost between that O-D pair under user equilibrium, which is depicted by a demand function. For NDP with elastic demand, the equilibrium travel demands between all O-D pairs and their traffic flow distribution on the network under a given capacity expansion plan can be obtained by solving the elastic-demand UE model.

In this work, the EUE model is used to depict traveler behavior and address the imbalance between transportation service supply and travel demand in the lower-level RPO problem formulation. As the event leads to a large-scale or severe degradation of road capacities within a short time period, a significant imbalance between travel demand and network capacity supply emerges. Moreover, travelers are more sensitive to road restoration status in the system within the RPO context. Therefore, although the time scale of RPO is relatively shorter than that of NDP, there is plenty of demand elasticity in the RPO problem. Hence, EUE is appropriate for modeling traveler behaviors and addressing the imbalance between supply and demand after a disruptive event.

The lower-level objective function of the RPO problem is shown in Equation (8). $D_{rs}^{-1}(\cdot)$ is the inverse of the monotonically decreasing demand function $D_{rs}(\cdot)$ between the O-D pair $r-s$.

The demand function relates the number of trips D_{rs} to the minimum travel time u_{rs} on the road network between r and s. The Elastic Exponential Demand Function is adopted in this work (SATURN, 2012):

$$D_{rs} = D_{rs}^{0} \exp\left(\beta\left(u_{rs}/u_{rs}^{0} - 1\right)\right) \tag{18}$$

D_{rs}^{0} and u_{rs}^{0} are defined as the travel demand and travel cost (minimum travel time in this work) between O-D pair r,s at a referencing scenario. The cost matrix is defined as costs with the unit of second. In a typical elastic traffic assignment model, it is widely accepted to select the $\left(D_{rs}^{0}, u_{rs}^{0}\right)$ at the base year where the demand matrix, road network topology, and link capacities are known, and the costs are acquired by user equilibrium accordingly. Thus, $\left(D_{rs}^{0}, u_{rs}^{0}\right)$ lies on both the supply curve and the demand curve. In this work, $\left(D_{rs}^{0}, u_{rs}^{0}\right)$ is selected as the corresponding variable at the user equilibrium before the event occurs.

Accordingly, the Inverse Demand Functions can be defined as:

$$u_{rs} = u_{rs}^{0} + \left(u_{rs}^{0}/\beta\right)\ln\left(D_{rs}/D_{rs}^{0}\right) \tag{19}$$

Similar to typical UE model, Equation (9) is an O-D flow conservation constraint. Equations (10) and (11) are non-negative constraints for path flows and O-D demand, and Equation (12) relates link flows to path flows through link-path incidence matrix.

4. Solution Algorithms for Proposed Bi-objective Bi-level Restoration Plan Optimization Problem

4.1. Solution Algorithm for Lower-level EUE Problem

In this subsection, a network representation method is proposed to solve the Elastic-demand UE problem. The traditional UE problem can be efficiently solved using the Frank-Wolfe method (Daskin and Sheffi, 1985). Sheffi summarized two different network representations that can be applied to transform the EUE problem to an equivalent traditional UE problem—zero-cost overflow formulation and excess-demand formulation (Daskin and Sheffi, 1985), as illustrated in Fig. 2(b) and Fig. 2(c), respectively. For the zero-cost overflow formulation, Fig. 2(b) shows a modification of the basic network in which every O-D pair is augmented to include a “dummy” origin node (designated r' in Fig. 2(b)). For the excess-demand formulation, the variable $f_{rs,p}$

denotes the excess demand, i.e., the trips cannot be accommodated between origin *r* and destination s ($f_{rs,p}$=$\bar{D}_{rs}-D_{rs}\left(u_{rs}\right)$). In this network representation, a pseudo link carrying the flow $f_{rs,p}$ is defined as directly connecting the origin to the destination for each O-D pair, as shown in Fig. 2(c) (Daskin and Sheffi, 1985).

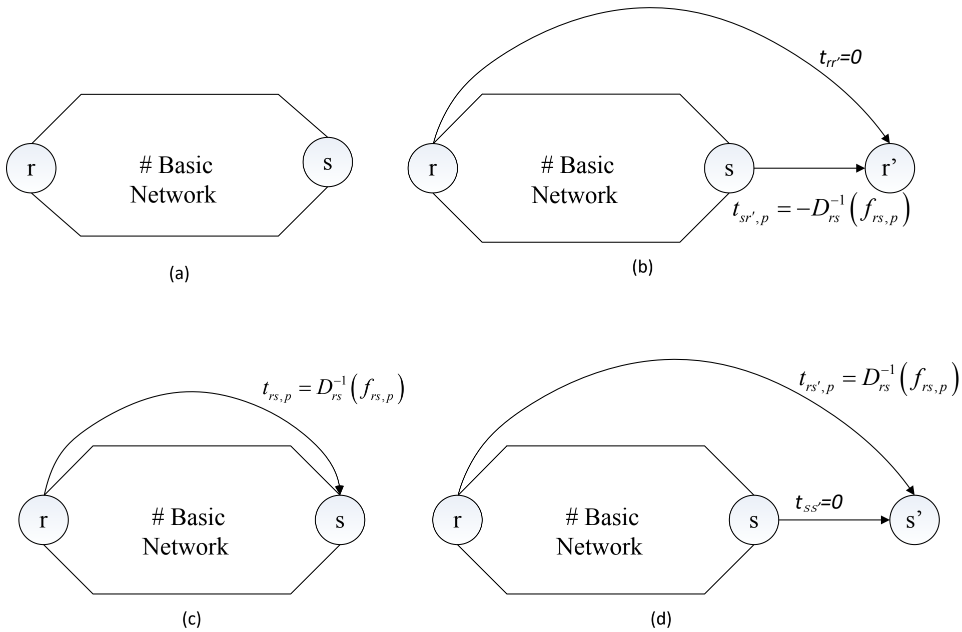

Fig. 2. Network representations: (a) basic network; (b) added node and links for O-D pair *r*-*s* in zero-cost overflow network representation; (c) excess-demand network representation for O-D pair *r*-*s*; (d) modified excess-demand network representation.

The excess-demand network representation is more straightforward for quantifying the unmet demand for resilience analysis of a transportation network. However, if there is a link connecting the origin to the destination of an O-D pair in the original network, it is necessary to distinguish the origin link a_{rs} and the pseudo link $a_{rs,p}$. Therefore, a "dummy" destination node is proposed (designated s' in Fig. 2(d)) for the excess-demand network representation. The new network representation—the modified excess-demand network representation—is illustrated in Fig. 2(d).

Therefore, the pseudo link cost-flow function is defined as follows to relate the cost $u_{rs,p}$ on the pseudo link to its flow $f_{rs,p}$.

$$u_{rs,p}=u_{rs}^{0}+\left(u_{rs}^{0}/\beta\right)\ln\left(\left(\bar{D}_{rs}-f_{rs,p}\right)/D_{rs}^{0}\right) \tag{20}$$

where $\bar{D}_{rs}$ is the total demand between O-D pair r,s before the special event. D_{rs}^{0} is a referencing point on the demand function, which is also chosen as the total demand between O-D pair r,s before the special event. Therefore, $\bar{D}_{rs}$ and D_{rs}^{0} have the same value in this study.

With the network representation and the link cost-flow function (i.e., inverse demand function) defined for the pseudo links, the EUE problem can be solved using the Frank-Wolfe algorithm.

4.2. Solution Algorithm for Single Objective Upper-level Restoration Plan Optimization Problem

The modified active set algorithm (Wang and Pardalos, 2017) is applied to solve the single objective upper-level optimization problem to minimize one of the two resilience measures or their combination. Binary variables $y_{a,l}, \forall a \in \bar{A}_1 \cup \bar{A}_2, l = 1,2$ are introduced to denote the control variables in the upper-level problem. $y_{a,l} = 1$ indicates that the corresponding plan is adopted, $y_{a,l} = 0$ otherwise, where a is the link index to perform this restoration and l is the indicator of two resource allocation levels. $l=1$ indicates restoration work with higher-level resource and more capacity restored, $l=2$ indicates lower-level resource assignment and less capacity restored.

Then, all binary variables $y_{a,l}$ are classified into two active sets:

$$\Omega_0 = \{(a,l): y_{a,l} = 0\} \tag{21}$$

$$\Omega_1 = \{(a,l): y_{a,l} = 1\} \tag{22}$$

The restoration work plan can be represented by these two active sets. Changing one or several (a,l) from Ω_0 to Ω_1 indicates a change in the restoration work plan. Then, constraints (4) and (5) of the upper-level problem can be reformulated as:

$$y_{a,l} = 0, \quad \forall (a,l) \in \Omega_0 \tag{23}$$

$$y_{a,l} = 1, \quad \forall (a,l) \in \Omega_1 \tag{24}$$

$g_{a,l}$ and $h_{a,l}$ are introduced to alter the representation of restoration work plan, Ω_0 and Ω_1. $g_{a,l} = 1$ means shifting (a,l) from Ω_0 to Ω_1, $h_{a,l} = 1$ means shifting (a,l) from Ω_1 to Ω_0. Then, the change of the upper level objective function is estimated by the following expression:

$$\sum_{(a,l)\in\Omega_0} \lambda_{a,l} g_{a,l} - \sum_{(a,l)\in\Omega_1} \mu_{a,l} h_{a,l} \tag{25}$$

where $\lambda_{a,l}$ and $\mu_{a,l}$ are the multipliers corresponding to constraints $y_{a,l} = 0$ and $y_{a,l} = 1$, respectively. $\lambda_{a,l}$ and $\mu_{a,l}$ can be calculated through:

$$\begin{cases} y_{a,l} = 0: \lambda_{a,l} = R' - R & \mu_{a,l} = 0 \\ y_{a,l} = 1: \lambda_{a,l} = 0 & \mu_{a,l} = R - R' \end{cases} \tag{26}$$

where R is the value of upper-level objective function before the change of Ω_0 and Ω_1. R' is the objective function value after the change, indicated by $g_{a,l}$ and $h_{a,l}$. Referring to Equation (27), R could be R_1 indicating Total Unmet Demand (*UMD*), R_2 indicating Total Travel Time (*TTT*) corresponding to two resilience measures, or the combination of them with more details explained at the end of Section 4.3.

After obtaining all feasible $(g_{a,l}, h_{a,l})$ pairs subject to Constraints (3)–(5) and corresponding changes of the upper-level objective function estimated by Equation (25), the $g_{a,l}$ and $h_{a,l}$ to reduce the resilience measure is found. Then, active sets Ω_0 and Ω_1 leading to the minimized upper-level objective function can be calculated iteratively. More details about the implementation procedure and the pseudo code of the modified active set algorithm can be found in Wang and Pardalos (2017).

4.3. Solution Algorithm for Bi-objective Optimization Problem

The weighted-sum method (Aneja and Nair, 1979) is adopted to find all supported non-dominated points for the overall bi-objective optimization problem. More details regarding this solution method are illustrated through the pseudo code and the step-by-step introduction. The basic idea is that firstly the two extreme endpoints R^T and R^B on the Pareto Frontier are obtained through solving the Lexicographic Optimality Problem (Ben-Tal, 1980). Then, by iteratively solving the following intermediate optimization problem to search a rectangle area defined by the extreme points R^1 and R^2 of the rectangle area, it can obtain all supported non-dominated points in the criteria space.

$$\min_{x \in \mathcal{X}} \{\lambda_1 R_1(x) + \lambda_2 R_2(x)\} \quad (27)$$

$$\text{subject to } R(x) \in Rec(\ R^1, R^2)$$

where $R_1(x)$ and $R_2(x)$ indicate two objective functions, i.e., minimizing two resilience measures; R^1 and R^2 indicate two extreme points; $Rec(\ R^1, R^2)$ indicates the rectangle with two extreme endpoints R^1, R^2 . The objective function of the intermediate problem is parallel to the line that connects the extreme points, R^1 and R^2, of the current rectangle area to be searched, $Rec(\ R^1, R^2)$, in the criterion space. Therefore, the weights to get the objective function of the intermediate problem are calculated as follows: $\lambda_1 = R_2^1 - R_2^2$ and $\lambda_2 = R_1^2 - R_1^1$, where R_2^1 indicates the second objective value for the extreme point R^1 , R_1^2 indicates the first objective value for the extreme point R^2 , etc.

Algorithm Weighted Sum Method

Procedure
Step 1. Compute endpoints R^T and R^B.
Step 2. Create list $List.create(L)$.
Step 3. Add points R^T and R^B to list *L*, $List.add(L, R^T)$, $List.add(L, R^B)$.
Step 4. Create queue *P* with rectangles to be searched, *PQ.create*(*P*). Add rectangle $Rec(R^T, R^B)$ to queue, $PQ.add(P, R(R^T, R^B))$.
Step 5. Optimize weighted sum single objective optimization problem $\min_{x \in \mathcal{X}} \{\lambda_1 R_1(x) + \lambda_2 R_2(x)\}$; if optimized point in criteria space satisfies criteria shown below, this point is newly-found non-dominated point that will separate the original rectangle to smaller rectangles to be searched. While queue is not empty, Step 5 will be performed iteratively.

```
while queue P is not empty, not PQ.empty(P) do
    PQ.pop(P, Rec(R^1, R^2))
    x* ← argmin_{x∈X} (R_2^1 − R_2^2)R_1(x) + (R_1^2 − R_1^1)R_2(x)
    R ← R(x*)
    if (R_2^1 − R_2^2)R_1 + (R_1^2 − R_1^1)R_2 < (R_2^1 − R_2^2)R_1^1 + (R_1^2 − R_1^1))R_2^1 then
        List.add(L, R)
        PQ.add(P, R(R^1, R))
        PQ.add(P, R(R, R^2))
return L
end while
end procedure
```

This intermediate optimization problem returns either one of R^1 and R^2 or a convex combination of R^1 and R^2. If the optimized result in the criteria space (R_1^{new}, R_2^{new}) satisfy the following criteria $\lambda_1 R_1^{new} + \lambda_2 R_2^{new} < \lambda_1 R_1^1 + \lambda_2 R_2^1$, the optimum point R^{new} is a newly found non-dominated point which will separate the original rectangle to smaller rectangles to be searched. The pseudo-code for the algorithm designed for the Bi-objective RPO problem is illustrated as follows.

Following the pseudo-code, the Weighted Sum Method can be implemented to solve the proposed bi-objective bi-level RPO problem, within which the intermediate problem $\min_{x \in X}\{\lambda_1 R_1(x) + \lambda_2 R_2(x)\}$ is solved by the modified active set algorithm and the network representation method introduced in Subsections 4.1 and 4.2. More specifically, the upper-level objective of the intermediate problem is min $R_1(x)$ when computing the endpoint R^T, min $R_2(x)$ when computing the endpoint R^B for solving the Lexicographic Optimality problem in Step 1, or min $\{\lambda_1 R_1(x) + \lambda_2 R_2(x)\}$ for solving the intermediate problem in Step 5.

5. Numerical Experiments

Numerical experiments are performed to demonstrate the validity, capability, and flexibility of the proposed bi-objective bi-level optimization model for solving the RPO problem. The proposed RPO method was applied to a typical road network in Sioux Falls, to illustrate the implementation procedures and verify the effectiveness of this method.

5.1. Sioux Falls Network and Damaged Links Selection (Failure Scenarios Generation)

The Sioux Falls network comprises 24 nodes and 76 links. In the topology shown in Fig. 3, 14 nodes marked in green serve as both origins and destinations in the system. In total, the network has 182 O-D pairs. The O-D trip matrix is referenced as Table 2 in Wang and Pardalos (2017), and the link capacity and free-flow travel time under normal conditions are referenced as Table 1 in Wang and Pardalos (2017).

The Sioux Falls network is a typical network in the existing literature, and there could be many different combinations of damaged links. To generate experimental scenarios with acceptable computing expense while reserving the diversity of the combinations of damaged links, 15 potentially damaged links in the system were selected as a subset of links from three different categories—edge links, links in the central area of the network, and links connecting the edge and the central area. As a result, links with indexes 1, 2, 4, 11, 13, 14, 17, 26, 27, 31, 36, 37, 39, 56, and 60 were chosen as the subset with 6 links (1, 2, 37, 39, 56, 60) at the edge of the network, 5 links (11, 13, 31, 26, 27) at the central area of the network, and 4 links (4, 14, 17, 36) connecting the edge and central areas of the network. This selection of potentially damaged links made it possible to represent different types of disruptive events, given that a hurricane or sea-level rise tend to induce capacity degradation at the edge of the network, an earthquake tends to cause collective disruption, and floods could affect a more disperse area. The selection of 15 potentially damaged links made it possible to generate various failure scenarios within this subset and to perform statistical analysis for the generated scenarios later. For each experimental scenario, N_{dam} links were randomly selected from the noted 15 links.

After a given disruptive event, the capacity of the selected link(s) was assumed to be decreased to 1/3 of the original link capacity. In other words, the damaged links were selected randomly, whereas the capacity deterioration ratio was deterministic in this work. Note that some disruptive events could cause the capacity degradation of some links and complete loss of capacity of some other links, i.e., the capacity deterioration ratios for links in the network could vary. The methodology proposed in this study could be applied to those experimental cases as well. Furthermore, it was assumed that the damaged links could be restored to two levels of capacity with corresponding two levels of restoration expenditure (see Table 2). This numerical experiment configuration enables verification of effectiveness and flexibility of the restoration plan optimization method proposed in Section 3 and Section 4.

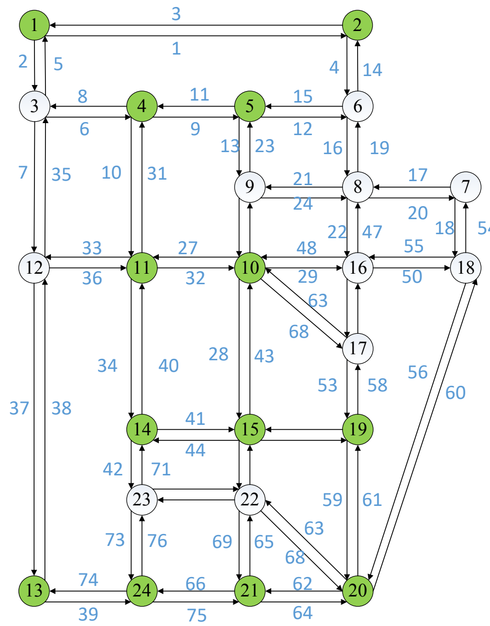

Fig. 3. Sioux Falls network topology.

Table 2 Potential damaged links and their repair costs.

Link index	**Free-flow travel time (min)**	**Capacity (10^3veh/h)**	**Cost1**	**Increased _capacity1**	**Cost2**	**Increased _capacity2**
1	3.6	6.02	8	6.02	4	4.01
2	2.4	9.01	8	9.01	4	6.01
4	3	15.92	14	15.92	7	10.61
11	1.2	46.85	32	46.85	16	31.23
13	3	10.52	10	10.52	5	7.01
14	3	9.92	10	9.92	5	6.61
17	1.8	15.68	12	15.68	6	10.45
26	1.8	27.83	20	27.83	10	18.55
27	3	20	16	20	8	13.33
31	3.6	9.82	10	9.82	5	6.55
36	3.6	9.82	10	9.82	5	6.55
37	1.8	51.8	34	51.8	17	34.53
39	2.4	10.18	10	10.18	5	6.79
56	2.4	8.11	8	8.11	4	5.41
60	2.4	8.11	8	8.11	4	5.41

***** Cost assumed as unit-less.

In the follow two subsections, the optimized solutions for a given failure scenario through criteria space analysis (see Section 5.2) are presented to demonstrate how the proposed method can support decision-making for road network restoration. Furthermore, to examine system performance enhancement after the restoration effort, an additional five groups of experiments were conducted assuming there are 1 to 5 links damaged, i.e., $N_{dam} = 1 \sim 5$ for each group, and three budget levels, *Budget*=15, 35, 55. As shown in Section 5.3, for all the scenarios, system resilience measures, both *TTT* and *UMD*, were computed before and after the restoration of infrastructure, as well as the corresponding restoration costs with optimal restoration plans.

5.2. Numerical Experiment Results

We take a specific failure scenario with links (1, 2, 4, 14) damaged as an example to show the bi-objective RPO optimization results and also to interpret the impact of budget level on the results. The feasible sets of the RPO problem with different budget levels are calculated. Then, the feasible solutions are shown in the criteria space with x-axis indicates the *UMD* and y-axis indicates the *TTT*. More specifically, for a feasible solution $Y = (\ldots, y_{a,l}, \ldots), \forall a \in \bar{A}_1 \cup \bar{A}_2, l = 1,2$ satisfying the budget constraint, we can obtain the corresponding *UMD* and *TTT* after restoration and then draw the solution points (*UMD, TTT*) in the criteria space accordingly. Fig. 4 (a) shows the feasible set enabled by different budget levels in the criteria space. The feasible set with higher budget F_{i+1} contains that with lower budget F_i. The feasible set enabled by additional budget is the difference between F_{i+1} and F_i. Suppose the feasible set enabled by budget level B_{i+1} is denoted as $\bar{F}_{i+1}$,then $\bar{F}_1 = F_1, \bar{F}_i = F_i - F_{i-1}, for\ i = 2\ldots5$. In Fig. 4, we plotted $\bar{F}_i, i = 1\ldots5$ with various colors indicating each $\bar{F}_i$. The circle marker indicates the points on the Pareto Frontier that can be found by the Weighted Sum Method. Due to the non-Convexity of the Pareto Frontier in criteria space, not all solution points on the frontier can be found.

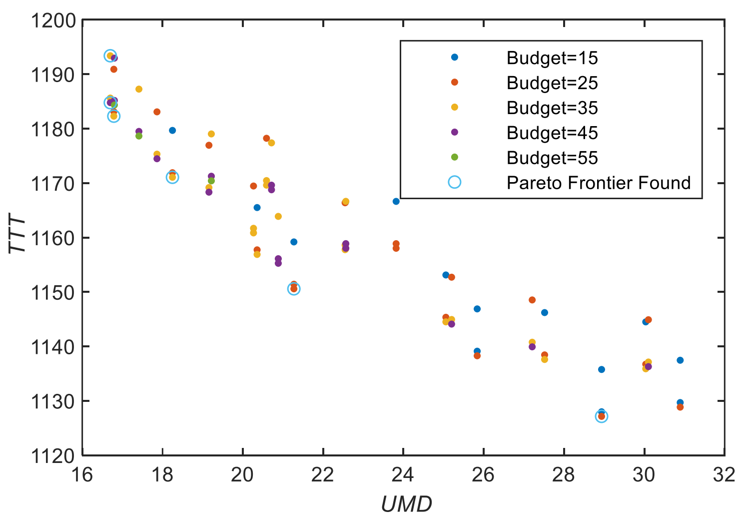

Fig. 4. Feasible solutions in criteria space enabled by different budget levels and solution points on Pareto Frontier found by Weighted Sum Method.

Fig. 5(a) and Fig. 5(b) shows Pareto Frontiers for *Budget=15* and *Budget=55,* respectively. It is observed that the two system performance metrics (*UMD* and *TTT*) contradict each other, and a higher budget level enables denser and better solutions on the Pareto Frontier. With *Budget=55,* more solutions with high *TTT* and low *UMD* are obtained, such as those in dashed-line circle at the upper left corner of Fig. 5(b).

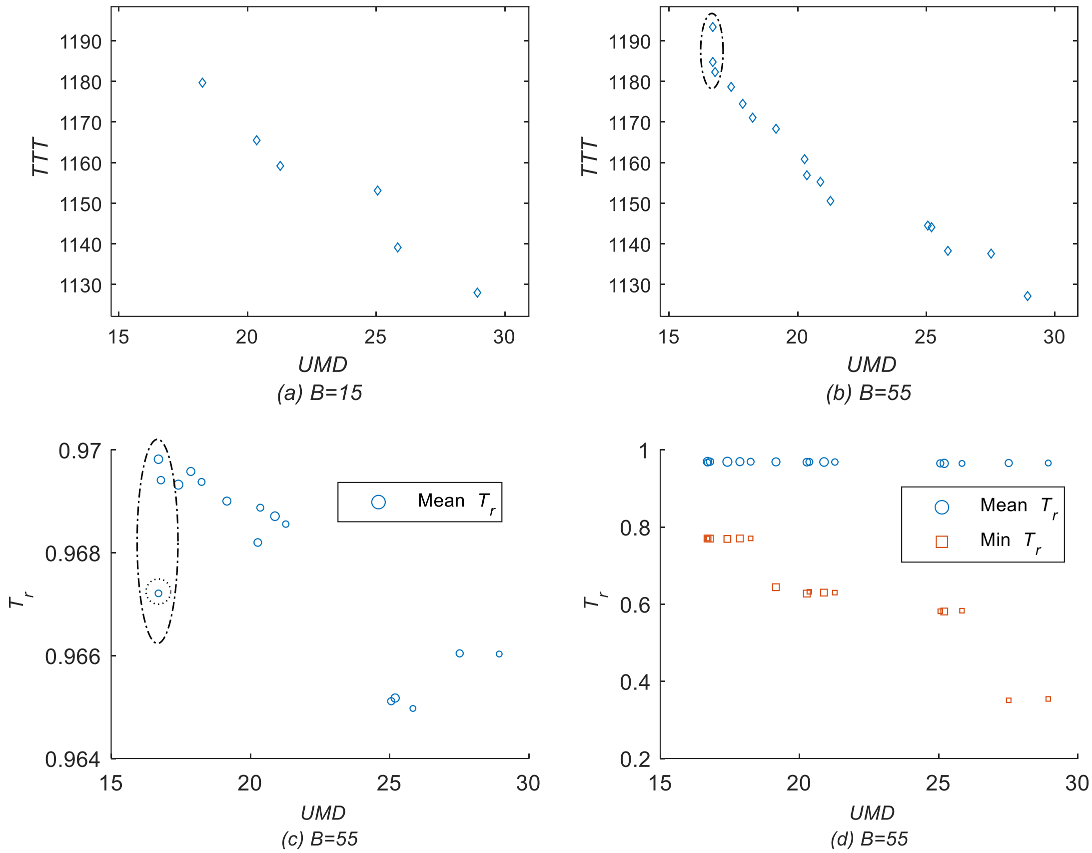

Fig. 5. Criteria space analysis (a) Pareto Frontier with *B=15*; (b) Pareto Frontier with *B=55*; (c) Mean T_r vs. *UMD* with *B=55*; (c) Min T_r vs. *UMD* with *B=55*.

Furthermore, we define travel time ratio $T_{r,a} = \frac{t_{0,a}}{t_a}$ to measure the efficiency of the system. For each link a, $t_{0,a}$ is the free flow travel time on link a and t_a is the travel time on link a after restoration. Given each restoration solution, Mean T_r and Min T_r, are calculated as follows:

$$\text{Mean } T_r = \frac{\sum_a T_{r,a}}{N_L}$$

$$\text{Min } T_r = \min(T_{r,a}), \quad a \in A$$

where A indicates the link set, $N_L = |A|$ is the number of links in the system. Higher Mean T_r indicates better "efficiency" on average for all trips in the system. Min T_r indicates worst case performance at single link level.

Then, we plot the Mean T_r and Min T_r vs. *UMD* in Fig. 5(c) and Fig. 5(d), respectively. The marker size in these two subfigures indicates the cost of the restoration plan for each solution. In Fig.5 (c), it is observed that the budget constraints are not always binding. The three solutions marked by the dash-dotted ellipse in Fig. 5 (b) and Fig. 5 (c) are corresponding to each other. Although the three solutions show similar *TTT* and *UMD* in Fig. 5(b), their Mean T_r is quite different. Thus, Mean T_r provides more information to decision makers. In Fig. 5(d), Min T_r vs.

UMD are plotted. Min T_r has larger variance over solutions, compared to Mean T_r. The solutions could be grouped to four clusters in terms of Min T_r, with larger *UMD* leading to lower Min T_r. Therefore, the solutions with less *UMD* can not only serve more travel demand but also improve the worst-case performance of the system. These observations show that the cross-reference among *TTT*, Mean T_r and Min T_r vs. *UMD* can help decision-makers compare the solutions through three different aspects, which leads to more comprehensive choice of restoration plan.

5.3 Statistical Analysis of Experiment Results for Various Failure Scenarios

More failure scenarios were generated to perform statistical analyses of the *TTT* and *UMD* before and after restoration work. For each failure scenario, we calculated the *TTT* and *UMD* before and after the restoration work, indicated as (T_0, $\hat{D}_0$) and (T_f, $\hat{D}_f$), respectively. There are $C_{15}^{5} = 3003$ cases when randomly selecting 5 links to be damaged from the 15 potential links. The box plot for the resilience measures, both *TTT* and *UMD* before and after restoration work and the cost-efficiencies of the restoration plan with 1–5 damaged links are shown in Fig. 6. As shown in Fig. 6(a) and 6(b), the median, upper quartile, and lower quartile of TTT_0 and TTT_f all monotonically decrease with the increased number of damaged links. Furthermore, the median, upper quartile, and lower quartile of TTT_f are larger than those of TTT_0. As shown in Fig. 6(c) and 6(d), the median, upper quartile, and lower quartile of UMD_0 and UMD_f all monotonically increase with the increased number of damaged links. The median, upper quartile, and lower quartile of UMD_f are smaller than those of UMD_0. These phenomena can be interpreted jointly with the observation in Fig. 4 showing that the two objectives, min *TTT* and min *UMD,* do contradict each other.

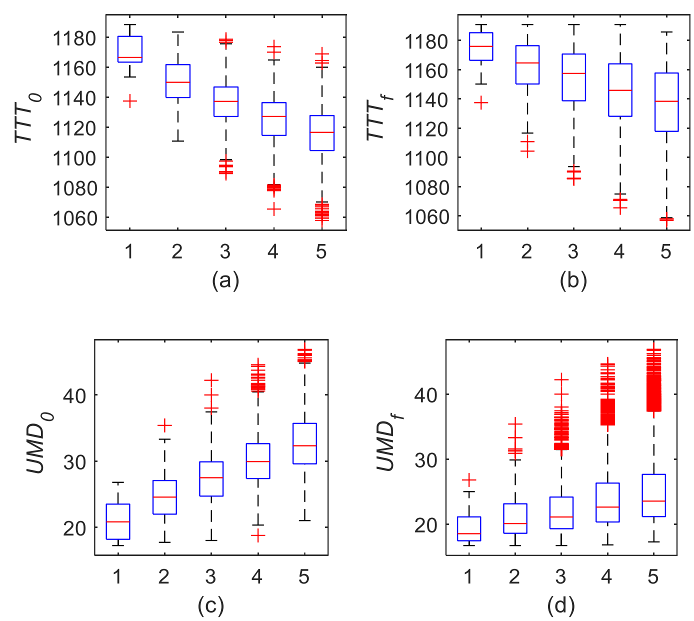

Fig. 6. Box plots of *TTT* before (a) and after (b) restoration and *UMD* before (c) and after (d) restoration

The two objectives, minimizing total unmet demand and total travel time provide decision-making support to choose an optimal restoration plan while balancing mobility and accessibility. As *TTT* and *UMD* have different units, we further define the total travel time reduced percentage, TTT_{Rd} (%), and the unmet demand reduced percentage, UMD_{Rd} (%), to better indicate the system performance in terms of two different measures in spite of their different units.

$$TTT_{Rd} = \frac{T_0 - T_f}{T_0} \qquad UMD_{Rd} = \frac{\hat{D}_0 - \hat{D}_f}{\hat{D}_0} \tag{28}$$

Fig. 7 shows the bivariate histograms of TTT_{Rd} and UMD_{Rd} with 4 or 5 links damaged in the system and budget levels of 15, 35, and 55. The motivation to do this visualization was to demonstrate how the optimized (TTT_{Rd}, UMD_{Rd}) jointly and statistically distributed over all the failure scenarios with N_{dam} links damaged and different budget levels. It is observed that with the increase of *Budget*, the grid cells with higher occurrence frequencies move from the lower right corner to the upper left corner, with the lower right corner indicating higher TTT_{Rd} and lower UMD_{Rd} and the upper left corner vice versa. Such observation means that with a higher budget, there are more optimized restoration plans that can reduce the unmet demand. Nevertheless, lower budget levels could also lead to diverse options in terms of trading off between TTT_{Rd} and UMD_{Rd}. This observed trend is even more clear with $N_{dam} = 5$ compared to those with $N_{dam} = 4$.

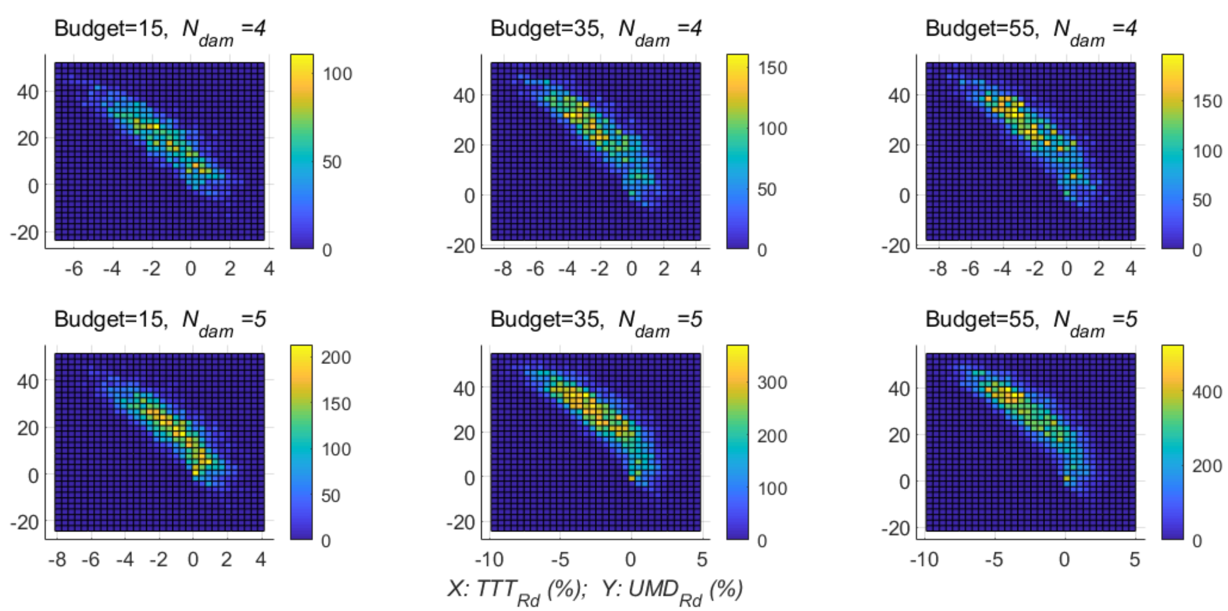

Fig. 7. Bivariate histogram of Reduced Percentages of *TTT* and *UMD* for $N_{dam} = 4$ and 5 and *Budget=15, 35, 55*. *X* axis indicates the *TTT* reduced percentage (%) after restoration. *Y* axis indicates the *UMD* reduced percentage (%) after restoration. Color bar indicates frequency of solutions' occurrence in this grid cell.

6. Conclusions

In this study, a roadway infrastructure restoration plan optimization method is proposed, formulated as a bi-objective bi-level optimization problem, to enhance system resilience performance in terms of total unmet demand and total travel time. This method makes it tractable to reduce not only total travel time from a mobility perspective but also unmet demand in a damaged system from an accessibility point of view. The bi-objective problem is solved by the Weighted Sum Method and by decomposing the problem into bi-level problems that are solved by a modified active set algorithm and a network representation method.

Numerical experiments were performed to demonstrate the validity, capability, and flexibility of the proposed bi-objective bi-level optimization model for solving the restoration plan. The restoration plan optimization method was applied to a typical road network to illustrate the implementation procedures and verify the effectiveness of the method. The criteria space analysis of one failure scenario demonstrates that two perspectives to measure system performance (*UMD* and *TTT*) contradict each other. Furthermore, travel time ratio, the ratio between free flow travel time and real travel time after restoration for each link, is defined and can provide further information to distinguish solutions that have similar performance in terms of *TTT* and *UMD*. The results demonstrate that cross-reference the travel time ratio with TTT and UMD can help decision-makers make more comprehensive solution choices. Furthermore, statistical analysis over five groups of failure scenarios were performed with 1–5 links damaged in the system. To address the different unit issue of *TTT* and *UMD*, we defined the reduced percentages of *TTT* and *UMD* compared with those before restoration. Bivariate histograms of the optimized reduced percentages of *TTT* and *UMD* are drawn to demonstrate how they are jointly and statistically distributed over all failure scenarios. The results show that although the lower budget could provide diverse solutions on the frontier trading off between reducing *TTT* and *UMD*, higher budget levels provide more options to further reduce *UMD*.

This study could be extended and strengthened in the following directions. First, it would be interesting to evaluate the performance of the proposed method on different typical road networks to validate some observations in this work. Second, given the outcomes from different representative road networks, a study could be conduct on if and how the network topology, design features, and demand distribution patterns of the system impact the optimal restoration plan and corresponding system resilience performance. This study focused on the resilience analysis of transportation systems without considering their interdependence with other CIs; a promising direction would be to model the interdependence between different CIs and propose effective decision-making support methodologies for restoration planning considering pooled budget and resource constraints for interdependent CIs.

ACKNOWLEDGMENTS

This research was supported by the National Science Foundation, CRISP Type 2: Integrative Decision-Making Framework to Enhance the Resiliency of Interdependent Critical Infrastructures. Award Number: 1638301, and the UTC CTEDD Seed Grant: Capacity-flow Feature-based Restoration Strategy Optimization for Resilient Transportation Systems to Enhance Mobility, Accessibility, and Equity after Disruptive Events, Project ID: 19-06 SG. The views, opinions, findings, and conclusions reflected in this paper are the responsibility of the authors only and do not represent the official policy or position of NSF or USDOT, or any other entity.

REFERENCES

Adams, T., Bekkem, K.R., Bier, V.M., 2011. Evaluating freight transportation resilience on a highway corridor. Transportation Research Board 90th Annual Meeting.

Adams, T.M., Bekkem, K.R., Toledo-Durán, E.J., 2012. Freight resilience measures. *Journal of*

Transportation Engineering, 138(11), 1403-1409.
Alderson, D.L., Brown, G.G., Carlyle, W.M., 2014. Assessing and improving operational resilience of critical infrastructures and other systems. *Bridging Data and Decisions*, INFORMS, 180-215.
Aneja, Y.P., Nair, K.P.K. 1979. Bicriteria transportation problem. *Management Science*, 25(1), 73-78.
Ben-Tal, A., 1980. Characterization of Pareto and lexicographic optimal solutions. In *Multiple Criteria Decision Making Theory and Application*, Springer, 1-11.
Boyce, D.E., Janson, B.N., 1980. Discrete transportation network design problem with combined trip distribution and assignment. *Transportation Research: Part B,* 14, 147-154.
Bretschneider, S., Kimms, A., 2011. A basic mathematical model for evacuation problems in urban areas. *Transportation Research Part A: Policy and Practice,* 45(6), 523-539.
Çelik, M., 2016. Network restoration and recovery in humanitarian operations: Framework, literature review, and research directions. *Surveys in Operations Research and Management Science,* 21(2), 47-61.
Chang, S.E., Nojima, N., 2001. Measuring post-disaster transportation system performance: The 1995 Kobe earthquake in comparative perspective. *Transportation Research Part A: Policy and Practice,* 35(6), 475-494.
Chen, L., Miller-Hooks, E., 2012. Resilience: An indicator of recovery capability in intermodal freight transport. *Transportation Science,* 46(1), 109-123.
Cova, T.J., Johnson, J.P., 2002. Microsimulation of neighborhood evacuations in the Urban-Wildland interface. *Environment and Planning A: Economy and Space,* 34(12), 2211-2229.
Cova, T.J., Johnson, J.P., 2003. A network flow model for lane-based evacuation routing. *Transportation Research Part A: Policy and Practice,* 37(7), 579-604.
Daskin, M.S., Sheffi, Y., 1985. *Urban Transportation Networks*. Prentice-Hall, Englewood Cliffs, New Jersey, USA.
Dixit, V., Wolshon, B., 2014. Evacuation traffic dynamics. *Transportation Research Part C: Emerging Technologies,* 49, 114-125.
Evans, A.W., 1992. Road congestion pricing: When is it a good policy?. *Journal of Transport Economics and Policy,* 213-243.
Faturechi, R., Miller-Hooks, E., 2014. Travel time resilience of roadway networks under disaster. *Transportation Research Part B: Methodological,* 70, 47-64.
Faturechi, R., Miller-Hooks, E., 2015. Measuring the performance of transportation infrastructure systems in disasters: A comprehensive review. *J. Infrastruct. Syst.*, 04014025.
Friesz, T.L., 1985. Transportation network equilibrium, design and aggregation: Key developments and research opportunities. *Transportation Research Part A: General,* 19(5-6), 413-427.
Gartner, N.H., 1980. Optimal traffic assignment with elastic demands: A review part I. Analysis framework. *Transportation Science*, 14(2), 174-191.
Gopalakrishnan, K., Peeta, S., 2010. *Sustainable and Resilient Critical Infrastructure Systems*. Springer.
Hai, Y., 1995. Sensitivity analysis for queuing equilibrium network flow and its application to traffic control. *Mathematical and Computer Modelling,* 22(4-7), 247-258.
Henry, D., Ramirez-Marquez, J.E., 2012. Generic metrics and quantitative approaches for system resilience as a function of time. *Reliability Engineering & System Safety,* 99, 114-122.
Jahangiri, A., Murray-Tuite, P., Machiani, S.G., Park, B., Wolshon, B., 2014. Modeling and assessment of crossing elimination for no-notice evacuations. *Transportation Research Record,* 2459(1), 91-100.
Leu, G., Abbass, H., Curtis, N., 2010. Resilience of ground transportation networks: A case study on Melbourne. 33rd Australasian Transport Research Forum.
Lim, E., Wolshon, B., 2005. Modeling and performance assessment of contraflow evacuation termination points. *Transportation Research Record,* 1922, 118-128.
Liu, P., Mu, D., 2015. Evaluating sustainability of truck weight regulations: A system dynamics view. *J. Ind. Eng. Management,* 8(5), 1711-1730.
Losada, C., Scaparra, M.P., O'Hanley, J.R., 2012. Optimizing system resilience: A facility protection model with recovery time. *European Journal of Operational Research,* 217(3), 519-530.
Miller-Hooks, E., Zhang, X., Faturechi, R., 2012. Measuring and maximizing resilience of freight

transportation networks. *Comput. Oper. Research,* 39, 1633.
Mingyuan, C., Attahiru Sule, A., 1991. A network design algorithm using a stochastic incremental traffic assignment approach. *Transportation Science*, 3, 215.
Morohosi, H., 2010. Measuring the network robustness by Monte Carlo estimation of shortest path length distribution. *Mathematics and Computers in Simulation,* 81(3), 551-559.
Murray-Tuite, P., Mahmassani, H., 2004. Transportation network evacuation planning with household activity interactions. *Transportation Research Record*, 1894, 150-159.
Murray-Tuite, P.M., 2006. A comparison of transportation network resilience under simulated system optimum and user equilibrium conditions. *Proceedings of the 38th Conference on Winter Simulation*, 1398-1405.
Naghawi, H., Wolshon, B., 2010. Transit-based emergency evacuation simulation modeling. *Journal of Transportation Safety & Security,* 2(2), 184-201.
Naghawi, H., & Wolshon, B. 2014. Operation of multimodal transport system during mass evacuations. *Canadian Journal of Civil Engineering,* 42(2): 81-88.
Nagurney, A., 2011. Building resilience into fragile transportation networks in an era of increasing disasters. 90th Annual Transportation Research Board Meeting.
Nogal, M., O'Connor, A., Caulfield, B., Martinez-Pastor, B., 2016. Resilience of traffic networks: From perturbation to recovery via a dynamic restricted equilibrium model. *Reliability Engineering & System Safety,* 156, 84-96.
Nogal, M., O'Connor, A., Martinez-Pastor, B., Caulfield, B., 2017. Novel probabilistic resilience assessment framework of transportation networks against extreme weather events. *ASCE-ASME Journal of Risk and Uncertainty in Engineering Systems, Part A: Civil Engineering*, 04017004.
Omer, M., Mostashari, A., Nilchiani, R., 2013. Assessing resilience in a regional road-based transportation network. *International Journal of Industrial and Systems Engineering,* 13(4), 389-408.
Righini, G., 2016. A network flow model of the Northern Italy waterway system. *EURO J. Transp. Logist.* 5(2), 99-122.
SATURN, 2012. Simulation and Assignment of Traffic in Urban Road Networks. *User Manual -Version 11.1*, March 2012
Siu, B.W., Lo, H.K., 2008. Doubly uncertain transportation network: Degradable capacity and stochastic demand. *European Journal of Operational Research,* 191(1), 166-181.
Soltani-Sobh, A., Heaslip, K., El Khoury, J., 2015. Estimation of road network reliability on resiliency: An uncertain based model. *International Journal of Disaster Risk Reduction,* 14, 536-544.
Taylor, M.A., 2012. Remoteness and accessibility in the vulnerability analysis of regional road networks. *Transportation Research Part A: Policy and Practice,* 46(5), 761-771.
Vugrin, E.D., Turnquist, M.A., Brown, N.J., 2014. Optimal recovery sequencing for enhanced resilience and service restoration in transportation networks. *International Journal of Critical Infrastructures* 10(3-4), 218-246.
Wang, X., Pardalos, P.M., 2017. A modified active set algorithm for transportation discrete network design bi-level problem. *Journal of Global Optimization*, 1-2, 325.
Waugh, W.L., 2000. *Living with Hazard: Dealing with Disasters. An Introduction to Emergency Management*. New York, ME Sharpe. Inc.
White House, The, 2013. Presidential Policy Directive–Critical Infrastructure Security and Resilience.
Wolshon, B., Zhang, Z., Parr, S., Mitchell, B., Pardue, J., 2015. Agent-based modeling for evacuation traffic analysis in megaregion road networks. *Procedia Computer Science,* 52, 908-913.
Wolshon, P.B., 2009. Transportation's role in emergency evacuation and reentry. Transportation Research Board, NCHRP Synthesis 392.
Xie, C., Lin, D.-Y., Travis Waller, S., 2010. A dynamic evacuation network optimization problem with lane reversal and crossing elimination strategies. *Transportation Research Part E: Logistics and Transportation Review,* 46(3), 295-316.
Xie, C., Turnquist, M., 2009. Integrated evacuation network optimization and emergency vehicle assignment. *Transportation Research Record,* 2091, 79-90.

Xie, C., Turnquist, M.A., 2011. Lane-based evacuation network optimization: An integrated Lagrangian relaxation and tabu search approach. *Transportation Research Part C: Emerging Technologies,* 19(1), 40-63.

Xu, X., Chen, A., Jansuwan, S., Heaslip, K., Yang, C., 2015. Modeling transportation network redundancy. *Transportation Research Procedia,* 9, 283-302.

Yang, H., H. Bell, M.G., 1998. Models and algorithms for road network design: A review and some new developments. *Transport Reviews,* 18(3), 257-278.

Yue, L., Zhenke, L., 2012. A bi-level model for planning signalized and uninterrupted flow intersections in an evacuation network. *Computer-Aided Civil and Infrastructure Engineering,* 27(10), 731-747.

Zhang, L., Lawphongpanich, S., Yin, Y., 2009a. An active-set algorithm for discrete network design problems. In Lam, W.H.K., Wong, S.C., Lo, H.K. (Eds.), *Transportation and Traffic Theory 2009: Golden Jubilee: Papers Selected for Presentation at ISTTT18*. Springer US, Boston, MA, 283-300.

Zhang, L., Wen, Y., Jin, M., 2009b. The framework for calculating the measure of resilience for intermodal transportation systems. National Center for Intermodal Transportation, No. 10-05-09.

Zhang, X., Miller-Hooks, E., Denny, K., 2015a. Assessing the role of network topology in transportation network resilience. *Journal of Transport Geography,* 46, 35-45.

Zhang, Z., Parr, S.A., Jiang, H., Wolshon, B., 2015b. Optimization model for regional evacuation transportation system using macroscopic productivity function. *Transportation Research Part B: Methodological,* 81, 616-630.

Zockaie, A., Mahmassani, H.S., Saberi, M., Verbas, O., 2014. Dynamics of urban network traffic flow during a large-scale evacuation. *Transportation Research Record*, 2422, 21-33.